



## Thermally-driven directional free-radical polymerization in confined channels

Journal:	<i>Polymer Chemistry</i>
Manuscript ID	PY-COM-10-2018-001550.R1
Article Type:	Communication
Date Submitted by the Author:	07-Jan-2019
Complete List of Authors:	Datta, Preeti; NC State, Chemical & Biomolecular Engineering Efimenko, Kirill; NC State, Chemical & Biomolecular Engineering; NC State University Genzer, Jan; North Carolina State University, Chemical and Biomolecular Engineering; North Carolina State University College of Natural Resources, Chemical & Biomolecular Engineering

## Thermally driven directional free-radical polymerization in confined channels

Preeta Datta<sup>†</sup>, Kirill Efimenko, Jan Genzer\*

Department of Chemical & Biomolecular Engineering  
North Carolina State University  
Raleigh, NC 27695-7905

We report on the formation of poly(acrylamide) (PAAm) with a relatively-narrow molecular weight distribution (MWD) by means of thermally-driven directional free-radical polymerization carried out in polymerization chambers featuring two parallel glass walls separated by various distances, ranging from sub-millimeter to a few millimeters. Using this experimental setup, in conjunction with size exclusion chromatography and peak fitting of MWD profiles of the resulting PAAm, we decouple two simultaneous modes of AAm polymerization reaction mechanisms, *i.e.*, thermal and monomer-initiated decompositions.

---

<sup>†</sup> Current address: Sealed Air Corporation, 2405 Cascade Pointe Blvd, Charlotte, NC 28208.

\* corresponding author: jgenzer@ncsu.edu

Key physical properties of polymers depend on the chemical nature of the monomeric units, the molecular weight and molecular weight distribution (MWD) of macromolecules, and the mechanism by which the polymers are formed.<sup>1</sup> While many polymers are synthesized in bulk, other modes of polymerization have also been employed, including, surface-initiated polymerization<sup>2-4</sup>, frontal polymerization,<sup>5-8</sup> grafting-through polymerization<sup>9,10</sup>, and others. In a typical frontal polymerization setup, a localized reaction front propagates in space and is driven by a complex interplay of Arrhenius kinetics and heat diffusion.<sup>11-15</sup> Here we use directional free-radical polymerization conducted between two parallel plates separated by sub- to millimeter spacings ( $H$ ). Specifically, we report on producing poly(acrylamide) (PAAm) with narrow molecular weight dispersity ( $\mathcal{D} \sim 1.2$ ) by confining thermal radical polymerization of acrylamide (AAM)<sup>16</sup>, irrespective of the location inside the reaction chamber or the degree of AAM conversion. The molecular weights of PAAm vary with  $H$  inside the reaction chamber away from the heating source. We demonstrate that varying  $H$  enables discriminating between two modes of AAM polymerization, i.e., monomer-enhanced decomposition and thermal decomposition, employing persulfate initiators (*vide infra*).

Our experimental set-up features a Teflon jacket of variable thickness that is sandwiched between two parallel insulating glass plates (*cf.* **Figure 1**) giving rise to a reaction chamber with adjustable  $H$  (see Supporting Information, SI, for details). To synthesize PAAm we use AAM, potassium persulfate, and dimethyl sulfoxide (DMSO) as the monomer, initiator and solvent, respectively. The polymerization reaction is initiated by placing a hot soldering iron along the edge of the reactor. Appearance of a white zone marks the occurrence of polymerization reaction. Three distinct regions appear as the polymerization reaction front propagates in space (*cf.* **Figure 1**). **Figure 1** displays the fractional monomer conversion along the direction of heat propagation, as measured by gas chromatography after polymerization.

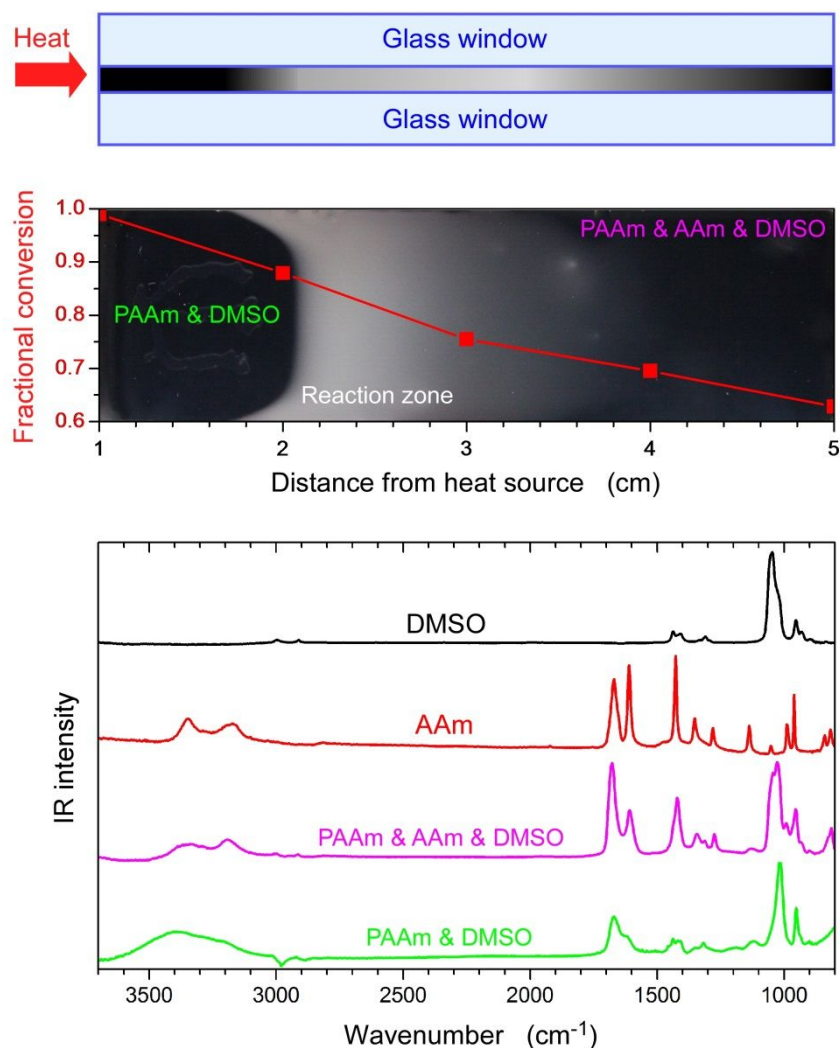


**Figure 1.** (top) Schematic depicting the side-view of the reaction set-up. (middle) The different reaction zones in thermally-driven directional polymerization with the respective monomer conversions. (bottom) IR spectra of dimethyl sulfoxide (DMSO), acrylamide (AAm) and the samples from the different zones.

The rate of polymerization of AAm varies non-linearly with AAm monomer concentration. To explain this unusual rate dependence of AAm polymerization, Hunkeler<sup>17</sup> proposed a "hybrid cage-complex" mechanism, in which hydrogen bonding between AAm and the initiator results in the formation of a charge-transfer complex. The decomposition of this complex leads to a secondary initiation reaction, which proceeds in competition with thermal bond rupture (often in preference) of the initiator. As a result, the polymerization of AAm using persulfate initiators undergoes either monomer-enhanced decomposition (MED) or conventional thermal decomposition (TD). The rates of polymerization are different for the two different modes of

initiation; *i.e.*,  $R \sim [M]$  (for TD) and  $[M]^{3/2}$  (for MED), where  $[M]$  is the monomer concentration. The two modes of polymerization lead to two MWDs of the products, which occur simultaneously; the overall rate of polymerization, according to Hunkeler, should be proportional to  $[M]^{5/4}$ . The observed 5/4th power for AAm polymerization is an "apparent" polymerization order, with the true kinetic process being a balance between the TD and MED mechanisms. Polymerization kinetics determines the molecular weight of the products as well as the MWD of PAAm.<sup>18</sup>

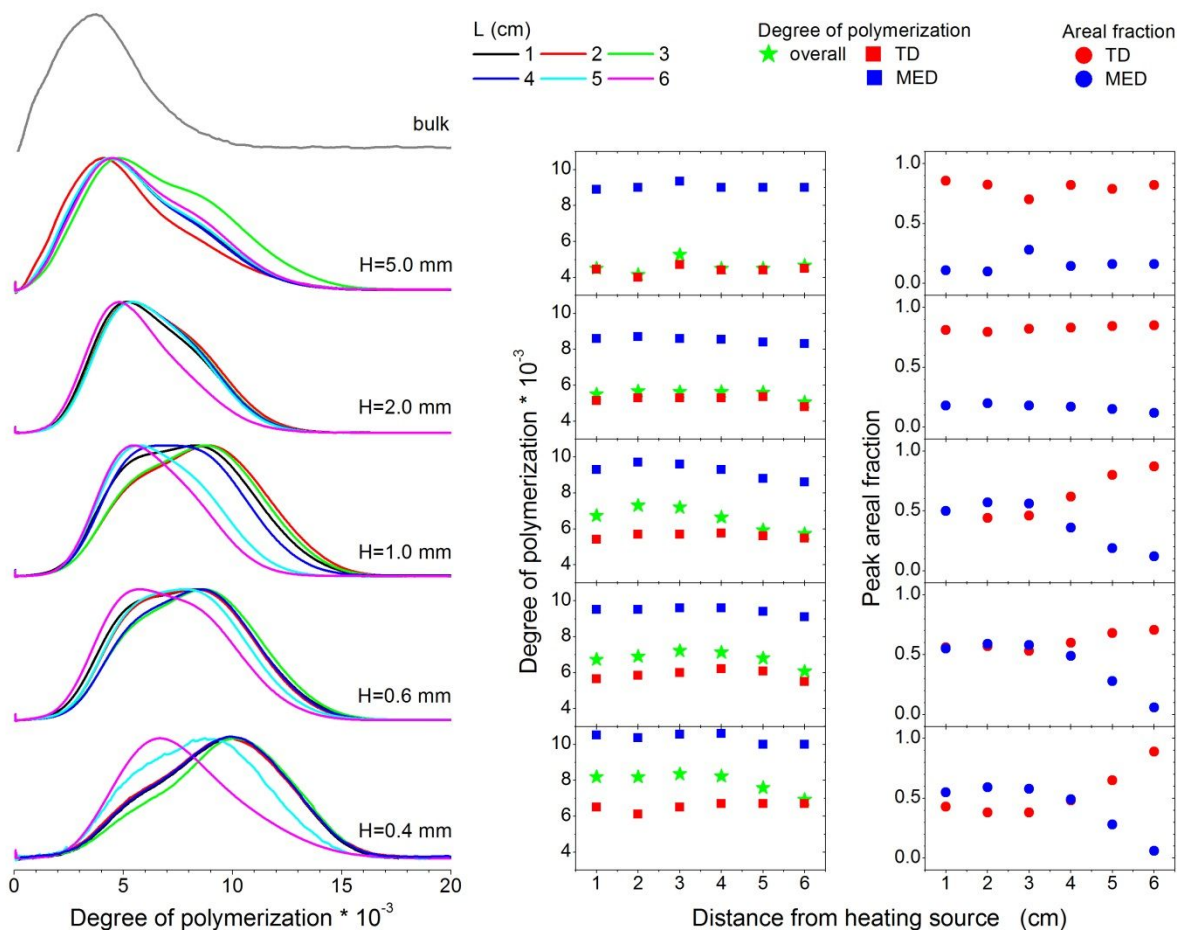


**Figure 2.** (Left panel) Experimental SEC elution curves collected from PAAm prepared in reactors featuring different reactor spacing ( $H$ ) and distances from the heating source ( $L$ ). (Right panels) Degrees of polymerization of the experimentally-determined overall molecular weight distribution (green stars) and most probable two distinct distributions (squares) as well as corresponding fractions (circles) of the thermal decomposition (TD, red data) and the monomer-enhanced decomposition (MED, blue data) mechanisms.

We let the polymerization front propagate for 60 mins under directional and constant heat supply. These experiments are carried out in reactors, whose  $H$  ranges from 0.4 to 2.0 mm. We

vary the ratio of initiator to monomer (*vide infra*). After quenching the reaction using liquid nitrogen and disassembling the reactor, we collect PAAm samples from different locations in the reaction chamber at equidistant intervals (1 cm) successively from the heat source for characterization using size exclusion chromatography (SEC). The left panel in **Figure 2** displays the SEC elution curves collected from PAAm that were prepared in reactors featuring different reactor spacings (H) and various distances from the heating source (L). The bimodal nature of the SEC curves (except for the bulk system) implies the presence of two distinct modes of polymerization. Specifically, we detect that in highly confined systems and close distances to the heating source, the high degree of polymerization mode (mode I) dominates, while at larger distances from the diffusing source and smaller confinement the lower degree of polymerization mode (mode II) takes over. We assign the mode I to MED and mode II to TD according to the discussion above and information provided in SI.

Each data set was rigorously fitted to two independent Schulz-Zimm MWDs, one for each mode; see SI for details. Iterative parameter fitting yields the degree of polymerization and fraction corresponding for each distribution (*cf.* right panel in **Figure 2**). As mentioned previously, the degree of polymerization depends on the degree of confinement and the distance from the heating source. For instance, PAAm polymerized in the confined reactor with  $H=0.4$  possesses degree of polymerization that is  $\sim 1.5$  times higher than that of PAAm prepared inside the  $H=2.0$  reactor and  $\sim 2.4$  times higher than that of PAAm prepared by conventional bulk free-radical polymerization. The contribution of the TD and MED modes depends on H. For  $H=0.4$  mm the MED dominates at short distances from the initiation center and eventually TD takes over at long distances from the heating source. For  $H=2.0$  mm the TD mode is the major governing mode of polymerization for all distances away from the heating source. AAm polymerization in reactors with  $H=0.4$  mm follows the “plug flow” mode while polymerization inside reactors having  $H \geq 2.0$  mm exhibits convection. The transition between the two modes takes place at approximately  $H > 1.0$  mm. We surmise this based on the images of the fronts published earlier in reference <sup>16</sup> and the MWD of PAAm and the deduced modes of polymerization shown in **Figure 2** in this paper. More details will be provided in a future publication.<sup>19</sup> Depending on the reactor spacing and the distance from the initiator site it is possible to decouple the two modes of polymerization reactions. As shown in **Figure 2**, in bulk polymerization TD is the predominant mode irrespective of the location within the reaction chamber.

We now proceed to deconvolute the effects of TD and MED on polymer MWD and  $\bar{D}$  in persulfate/AAM systems. We vary the initiator to AAM monomer ratio progressively from 1:75, 1:750 to 1:1500 for  $H=0.4$  mm and  $H=2.0$  mm. Temperature profiles inside the reactor at regular time intervals (red dotted lines in **Figure 3**) are determined by measuring the temperature of the upper glass surface with an IR camera and calculating temperature inside the reactor via a conductive heat transfer model (see SI for details). The heat loss in a “highly” confined (*i.e.*,  $H=0.4$  mm) system is much higher than that in a reaction chamber with  $H=2$  mm. Since such directional polymerization propagates via a positive feedback mechanism with respect to thermal energy, a greater heat loss translates into slower reaction kinetics and lower overall heat generation. As a result, there is a clear difference in the local temperatures at all distances away from the heat source across  $H=0.4$  and  $H=2$  mm, demonstrated in **Figure 3**. The temperature gradients are higher in the less confined systems; more initiators with lower half-life times are activated and polymerization progresses rapidly thus generating more heat of reaction which further increases the temperature gradients. In addition, the occurrence of convection in high  $H$  can distort the reaction front and lead to mixing inside the reaction chamber, thus approaching bulk reaction behavior (*cf.* **Figure 3**).<sup>18-25</sup> Convection assists in faster front propagation; it increases thermal transport and the front velocity and may cause depletion of monomers in the front region. In a highly confined system (*i.e.*,  $H=0.4$  mm), lower temperature gradients lead to more controlled initiation and chain growth, *i.e.*, fewer initiators with longer half-lives are activated and the chains grow relatively slowly. The temperature uniformity inside the reaction chamber at all times indicates that chain propagation occurs at roughly the same temperature in more confined systems. As a result, the polymer product possesses high molecular weight and low  $\bar{D}$  relative to less confined systems where polymerization proceeds faster. Physical gelation present during polymerization narrows down the MWD of polymers due to decreased mobility of the growing chains, which minimizes the likelihood of termination. We attribute the low  $\bar{D}$  dispersity values to the simultaneous contribution of slow front propagation velocity, the suppression of convection in vertically confined systems, and the gelation effect. More details will be provided in a future publication.<sup>19</sup>

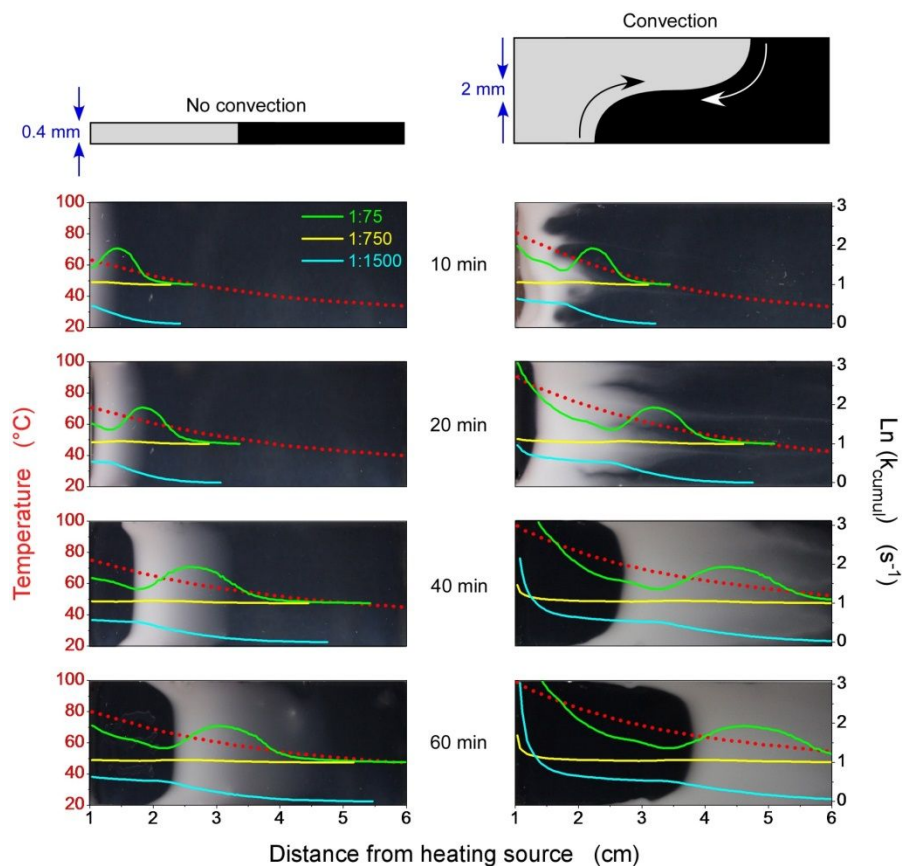


**Figure 3.** Cumulative rate constants for different initiator to monomer ratios measured by differential scanning calorimetry, superposed on the top view of a propagating reaction front as a function of distance from the heating source (L) for two different reactor spacings:  $H=0.4$  mm (left) and  $H=2.0$  mm (right). The photographs correspond to the green lines in the figure. The schematic (top) illustrates how convection in less confined systems can lead to bulk-like mixing and resulting distortion of the otherwise sharp reaction interface.

To identify the reaction kinetics of the TD and MED distributions (shown in red and blue in the right panel in **Figure 2**), we performed differential scanning calorimetry (DSC) measurements on acrylamide/dimethyl sulfoxide mixtures of different compositions with varying amounts of persulfate initiator. By fitting the DSC data to Arrhenius kinetics, we determined the associated rate constants as a function of temperature and plotted the rate constants as a function of distance from the heat source (*cf.* **Figure 3**, see SI for details). The rate constant determined from the DSC measurements represents a lumped rate constant, for both TD and MED modes, given the highly exothermic nature of AAm polymerization.<sup>26-30</sup> For low persulfate to acrylamide ratio (*i.e.*, 1:1500), *i.e.*, in the presence of excess AAm monomer, the predominant mode of polymerization is MED and the cumulative rate constant exhibits a gradual decrease along the

direction of heat propagation, *i.e.*, with decreasing temperature (*cf.* **Figure 3**). For high initiator to monomer ratio (*i.e.*, 1:75), ahead of the sharp interface that marks the reaction front, the cumulative rate constant increases with increasing temperature to reach a maximum value and then decreases. At intermediate values of initiator to monomer ratios (*i.e.*, 1:750), the cumulative rate constant values reside between the two extremes and do not exhibit much variation with temperature. Convection accelerates and distorts the propagating reaction front, as in H=2 mm reactor data plotted in **Figure 3**. Additionally, net heat accumulation is greater in H=2 mm thick reactor than the H=0.4 mm reactor, as the ratio of surface to volume, and therefore the ratio of heat generation to heat loss, is lower. The cumulative effect of convection and low surface-to-volume ratio leads to a shift in the rate constants for the less confined system (H=2 mm) at any given time.

We reconcile our observations as follows. The rate constant associated with TD is higher than that corresponding to MED at any given temperature. As a result, TD contributes substantially to the overall polymerization. Because the rate of polymerization varies as  $[M]$  for TD, the kinetic chain length, and therefore the molecular weight of the corresponding products, is lower relative to the MED mode, for which the rate of polymerization varies as  $[M]^{3/2}$  (see SI). Because of convection-driven kinetics in less confined systems (*i.e.*, higher H), monomer is depleted faster at any given location and therefore the rate of chain propagation and the average molecular weight of the MED products (blue population) is lower than in case of more confined systems (*i.e.*, H=0.4 mm).

A confined polymerization reactor can be thought of as a series of plug-flow reactors with negligible mixing. Each position along the direction away from the heat source possesses different kinetic history and corresponds to different stages of monomer conversion. Polymers synthesized by thermally-driven directional free-radical polymerization under confinement exhibit exceptionally narrow MWD. Under high degree of confinement such polymerization enables separating two distinct modes of polymerization of AAm in a spatio-temporal manner.

### Conflicts of interest

There are no conflicts to declare.

### Author information

\*Email: [jgenzer@ncsu.edu](mailto:jgenzer@ncsu.edu)

ORCID: Preeti Data: 0000-0003-1078-1915

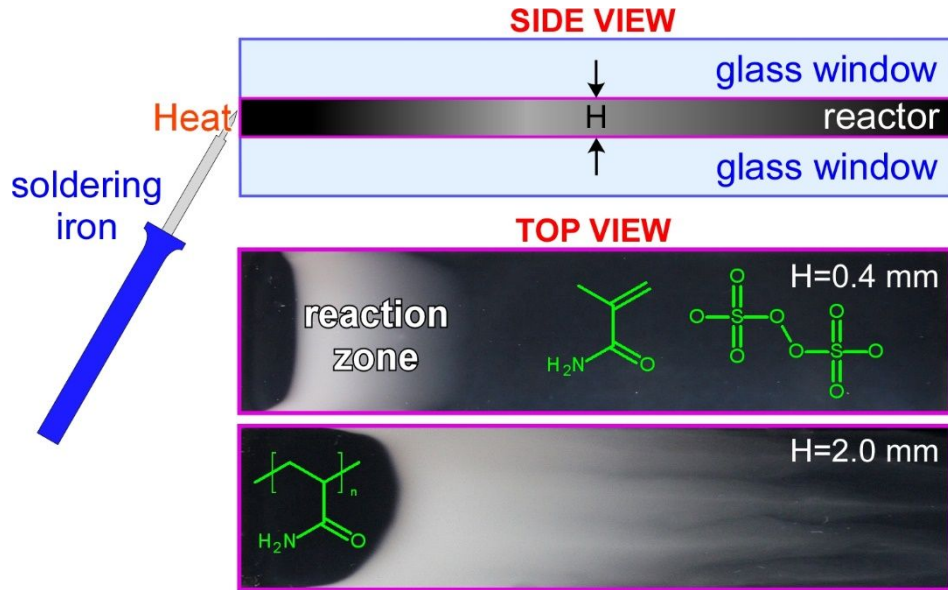
ORCID: Kirill Efimenko: 0000-0002-6777-7266

ORCID: Jan Genzer: 0000-0002-1633-238X

### **Acknowledgements**

We thank the National Science Foundation (grant No. CBET-0853667) for supporting the work and Prof. Saad Khan (NC State) for access to DSC in his laboratory.

TOC figure



## References

- 1 G. Odian, *Principles of polymerization*, John Wiley & Sons: Hoboken, 2004.
- 2 J. Zhao, W.J. Brittain, W.J., "Polymer brushes: surface-immobilized macromolecules", *Prog. Polym. Sci.* 2000, **25**, 677-710.
- 3 B. Brittain, R. Advincula, J. R uhe, and K. Caster (Eds.), *Polymer Brushes*, Wiley & Sons, 2004.
- 4 O. Azzaroni, I. Szleifer, editors. *Polymer and Biopolymer Brushes: Fundamentals and Applications in Materials Science and Biotechnology*, Wiley, 2017.
- 5 J.A. Pojman, "Frontal Polymerization", in *Encyclopedia of Polymer Science: A comprehensive reference*, K. Matyjaszewski & M. M oller, (Eds.), Amsterdam, Vol. 4, pp. 957, 2012.
- 6 J. A. Pojman, D. Fortenberry and V. Ilyashenko, Frontal polymerization as an analog of SHS. *Int. J. Self-Propag. High-Temp. Synth.* 1997, **6**, 355-376.
- 7 J.A. Pojman, J. Masere, E. Petretto, M. Rustici, D.S. Huh, M.S. Kim and V. Volpert, The effect of reactor geometry on frontal polymerization spin modes. *Chaos* 2002, **12**, 56-65.
- 8 J.A. Pojman, Traveling fronts of methacrylic acid polymerization. *J. Am. Chem. Soc.*, 1991, **113**, 6284-6286.
- 9 P.M. Goldfeder, V.A. Volpert, V.M. Ilyashenko, A.M. Khan, J.A. Pojman and S.E. Solov'yov, Mathematical modeling of free-radical polymerization fronts. *J. Phys. Chem. B* 1997, **101**, 3474-3482.
- 10 D. Henze, O. Madge, O. Prucker and J. R uhe, "'Grafting Through': Mechanistic Aspects of Radical Polymerization Reactions with Surface-Attached Monomers", *Macromolecules* 2014, **47**, 2929-2937.
- 11 P. Datta, J. Genzer, "Grafting Through" Polymerization involving surface-bound monomers", *J. Polym. Sci. Part A: Polym Chem.* 2015, **54**, 263-274.
- 12 J.A. Pojman, J. Willis, D. Fortenberry, V. Ilyashenko, and A. Khan, Factors affecting propagating fronts of addition polymerization: Velocity, front curvature, temperature profile, conversion and molecular weight distribution. *J. Polym. Sci. Part A: Polym Chem.* 1995, **33**, 643-652.
- 13 M. Bazile Jr., H.A. Nichols, J.A. Pojman and V. Volpert, The effect of orientation on thermoset frontal polymerization. *J. Polym. Sci. Part A: Polym Chem.* 2002, **40**, 3504-3508.
- 14 R.P. Washington and O. Steinbock, Frontal polymerization synthesis of temperature-sensitive hydrogels," *J. Am. Chem. Soc.* 2001, **123**, 7933-7934.

- 15 A. Vitale, M. G. Hennessy, O.K. Matar and J.T. Cabral, Interfacial Profile and Propagation of Frontal Photopolymerization Waves. *Macromolecules* 2015, **48**, 198–205.
- 16 P. Datta, K. Efimenko and J. Genzer, Effect of confinement on thermal frontal polymerization. *Polymer Chemistry* 2012, **3**, 3243-3246.
- 17 D. Hunkeler, Mechanism and kinetics of the persulfate-initiated polymerization of acrylamide. *Macromolecules* 1991, **24**, 2160-2171.
- 18 D. Colombani, Chain-growth control in free radical polymerization. *Progress in Polymer Science* 1997, **22**, 1649-1720.
- 19 P. Datta and J. Genzer, in preparation (2019).
- 20 V. Volpert, V.A. Volpert, J.A. Pojman and S.E. Solovyov, Hydrodynamic stability of a polymerization front. *Eur. J. Appl. Math.* 1996, **7**, 303-320.
- 21 J.A. Pojman, R. Craven, A. Khan and W. West, Convective instabilities induced by traveling fronts of addition polymerization. *J. Phys. Chem.* 1992, **96**, 7466-7472.
- 22 J.A. Pojman, V.M. Ilyashenko and A.M. Khan, Spin mode instabilities in propagating fronts of polymerization. *Physica D* 1995, **84**, 260-268.
- 23 B. McCaughey, J.A. Pojman, C. Simmons and V.A. Volpert, The effect of convection on a propagating front with a liquid product: Comparison of theory and experiments. *Chaos* 1998, **8**, 520-529.
- 24 G. Bowden, M. Garbey, V.M. Ilyashenko, J.A. Pojman, S. Solovyov, A. Taik and V. Volpert, The effect of convection on a propagating front with a solid Product: Comparison of theory and experiments. *J. Phys. Chem. B* 1997, **101**, 678-686.
- 25 V.A. Volpert, V.A. Volpert and J.A. Pojman, Effect of thermal expansion on stability of reaction front propagation," *Chem. Eng. Sci.* 1994, **14**, 2385-2388.
- 26 H.Y. Zhao, Z.N. Yu, F. Begum, R.C. Hedden and S.L. Simon, The effect of nanoconfinement on methyl methacrylate polymerization:  $T_g$ , molecular weight, and tacticity. *Polymer* 2014, **55**, 4959-4965.
- 27 F. Begum, H.Y. Zhao and S.L. Simon, Modeling methyl methacrylate free radical polymerization: Reaction in hydrophobic nanopores. *Polymer* 2012, **53**, 3261 – 3268.
- 28 M.B. Wisnudel and J.M. Torkelson, Diffusion-limited photophysical interactions as in situ probes of conversion in free radical polymerization: Quantitative analysis with predictive free-volume theory. *Macromolecules* 1994, **27**, 7217-7225.

- 29 R.G.W. Norrish and R.R. Smith, Catalyzed polymerization of methyl methacrylate in liquid phase. *Nature* 1942, **150**, 336-337.
- 30 V.F. Kurenkov and L.I. Abramova, Homogeneous polymerization of acrylamide in solutions. *Polym. Plast. Technol. Eng.* 1992, **31**, 659-704.